Multi-biomarker pharmacokinetic-pharmacodynamic relationships of central nervous systems active dopaminergic drugs

Brink, W.J. van den

CHAPTER 6

MULTIVARIATE PHARMACOKINETIC/ PHARMACODYNAMIC (PKPD) ANALYSIS WITH METABOLOMICS SHOWS MULTIPLE EFFECTS OF REMOXIPRIDE IN RATS

WJ van den Brink, J Elassaiss-Schaap, B Gonzalez-Amoros, AC Harms, PH van der Graaf, T. Hankemeier, ECM de Lange

Published in European Journal of Pharmaceutical Sciences 2017 109:431-440

Abstract

The study of central nervous system (CNS) pharmacology is limited by a lack of drug effect biomarkers. Pharmacometabolomics is a promising new tool to identify multiple molecular responses upon drug treatment. However, the pharmacodynamics are typically not evaluated in metabolomics studies, although being important properties of biomarkers.

In this study we integrated pharmacometabolomics with pharmacokinetic/pharmacodynamic (PKPD) modeling to identify and quantify the multiple endogenous metabolite dose-response relations for the dopamine D2 antagonist remoxipride.

Remoxipride (vehicle, 0.7 or 3.5 mg/kg) was administered to rats. Endogenous metabolites were analyzed in plasma using a biogenic amine platform and PKPD models were derived for each single metabolite. These models were clustered on basis of proximity between their PKPD parameter estimates, and PKPD models were subsequently fitted for the individual clusters. Finally, the metabolites were evaluated for being significantly affected by remoxipride.

In total 44 metabolites were detected in plasma, many of them showing a dose dependent decrease from baseline. We identified 6 different clusters with different time and dose dependent responses and 18 metabolites were revealed as potential biomarker. The glycine, serine and threonine pathway was associated with remoxipride pharmacology, as well as the brain uptake of the dopamine and serotonin precursors.

This is the first time that pharmacometabolomics and PKPD modeling were integrated. The resulting PKPD cluster model described diverse pharmacometabolomics responses and provided a further understanding of remoxipride pharmacodynamics. Future research should focus on the simultaneous pharmacometabolomics analysis in brain and plasma to increase the interpretability of these responses.

Keywords: Systems pharmacology; PK/PD modeling; pharmacometabolomics; biomarkers; CNS drugs; D2R antagonists

Abbreviations

AAAD: Aromatic Amino Acid Decarboxylase; AQC: 6-AminoQuinolyl-N-hydroxysuccinimidyl Carbamate; ASCA: Anova Simultaneous Component Analysis; BCAA: Branched Chain Amino Acids; brainECF: Brain extracellular fluid; CNS: Central Nervous System; D2R: dopamine D2 Receptor; DOPAC: 3,4-dihydroxyphenylacetic acid ; FWER: Family Wise Error Rate; HVA: Homovanillic acid; L-DOPA: L-3,4-dihydroxyphenylalanine; MeOH: Methanol; MS: Mass Spectometry; NMDA: N-Methyl-D-Aspartate; OFV: Objective Function Value; PCA: Principal

Component Analysis; PD: Pharmacodynamics; PK: Pharmacokinetics; PLS-DA: Partial Least Squares Discriminant Analysis; QC: Quality Control; RSD: Relative Standard Deviation; RSE: Relative Standard Error; RV: Residual Variability; SRM: Single Reaction Monitoring; TCEP: Tris(2-CarboxyEthyl)Phosphine; UPLC: Ultra high Performance Liquid Chromatography; VIP: Variable Importance Projection; WCSS: Weighted Cumulative Sum of Squares

Introduction

Central nervous system (CNS) drug development is difficult and attrition rates are high [1]. While important progress has been made in the insight into human brain pharmacokinetics (PK) in response to plasma PK, insights into the relation to the time dependent CNS drug effects are limited [2–4]. It is therefore essential to utilize biomarkers that provide proof of pharmacology and dosing guidance for early clinical drug development [2,4–9]. Preferably, these biomarkers are measured in the blood, since blood can be easily obtained from humans.

Biomarker discovery is increasingly driven by (pharmaco)metabolomics [10–15]. It measures the end-products of cellular biochemical reactions under a drug-perturbed, disease or control condition, and is as such a phenotypic measure, sometimes referred to as the "metabotype" [16]. As an example, a pharmacometabolomics approach has been successfully applied in CNS drug research for identification of serum biomarkers of antipsychotic drug efficacy [17] or toxicity [18].

An important limitation so far has been that pharmacometabolomic studies are often performed at single time points while many biological processes change with time. A single time point evaluation thus limits the ability to accurately quantify the extent and duration of drug effects. Whereas for single time point studies multivariate data analysis mostly is performed using principal component analysis (PCA) and partial least squares discriminant analysis (PLS-DA) [19], more advanced methods are needed, and have been developed, to evaluate time-dependent effects in metabolomics data. For example, an extension of PCA was developed called ANOVA Simultaneous Component Analysis (ASCA), allowing for multivariate evaluation in multiple dimensions (e.g. dose, time and response) [20]. Still, a remaining limitation with this method is that the variables are treated as categorical data, while factors as dose and time typically are continuous variables. Furthermore, longitudinal clustering approaches are promising for the evaluation of multivariate longitudinal data, although its application until now has been mainly on gene expression data [21–24].

Not only the time course of the effect biomarker is important for the understanding of drug effects, but also the causal relation between drug dose and biomarker response

(Danhof et al. 2005). This relation is governed by processes of drug distribution to the target site [2,25], receptor binding [26] and activation [27], signal transduction [23,27] and homeostatic feedback [28]. These processes are typically non-linear, which increases the complexity from a data analysis perspective. Quantitative insights in drug effects are obtained by a combination of studies that measure biomarkers at different causal levels in a time-dependent manner and pharmacokinetic/pharmacodynamic (PKPD) modeling [2,5,29–31].

In this study we integrated pharmacometabolomics with PKPD modeling to identify and quantify multiple endogenous metabolite dose-response relations for the paradigm compound remoxipride. Rats received remoxipride in different dose levels and we obtained serial plasma samples for analysis of multiple endogenous metabolites. PKPD models were subsequently developed to fit the longitudinal dose-response data of each single metabolite. Biomarker clusters were identified on basis of the PKPD parameters to derive a PKPD model that fitted the cluster responses. Potential biomarkers and putative pharmacological pathways of remoxipride effect were identified using this approach; we obtained comprehensive insight in its differential effects on the endogenous metabolism.

Methods

Animal studies

Animal studies were performed in agreement with the Dutch Law of Animal Experimentation and approved by the Animal Ethics Committee in Leiden, the Netherlands (study protocol DEC13186). Male Wistar rats (n= 28, 278 +/- 15 g, Charles River, The Netherlands) were housed in groups for 6-9 days until surgery (Animal Facilities Gorlaeus Laboratories, Leiden, The Netherlands). Animals were held under standard environmental conditions while artificial daylight was provided from 7:30AM to 7:30PM. They had ad libitum access to food (Laboratory chow, Hope Farms, Woerden, The Netherlands) and acidified (to prevent infection) water.

Surgery and experiment

Surgery was done according to previously reported procedures [25]. In brief, animals received 2% isoflurane anesthesia while undergoing surgery. Cannulas were placed in the femoral artery for serial blood sampling and the femoral vein for drug administration. Microdialysis guides (CMA 12 Elite PAES, Schoonebeek, The Netherlands) were placed in caudate putamen (AP −1.0; L 3.0; V −3.4, relative to bregma) and replaced by microdialysis probes (CMA 12 Elite PAES, 4 mm polycarbonate membrane, cut-off 20 kDA, Schoonebeek, The Netherlands) before the experiment. For 7 days, animals were individually held in Makrolon type 3 cages to recover from surgery. The start of the experiments was between

8:00AM and 8:30AM and rats were randomly assigned receiving 0 mg/kg (n=5), 0.7 mg/kg (n=8), or 3.5 mg/kg (n=9) remoxipride by i.v. bolus (2 min infusion) at the start of experiment (t=0 min). Microdialysis was performed using buffered perfusion fluid and a flow rate of 1µl/min. Blood samples of 200 µl were collected in heparin-coated eppendorf tubes at -15, 2, 10, 22, 30, 40, 60, 100, 180 and 240 min, after which animals received 200 ul saline to compensate for the lost blood volume. Plasma was separated by centrifuging (1000 g, 10 min) and was stored at 4°C during the experiment and at -20°C after the experiment until analysis.

Metabolomics analysis

Metabolomics analysis in the plasma samples was performed using an amine platform, according to a previously described method [32]. The amine platform covers amino acids and biogenic amines employing an Accq-tag derivatization strategy adapted from the protocol supplied by Waters (Etten-Leur, The Netherlands). 5 µL plasma was spiked with an internal standard solution and reduced with TCEP (tris(2-carboxyethyl)phosphine) followed by deproteination by addition of MeOH. After centrifuging (9400xg, 10 min, 10°C), the supernatant was transferred to a deactivated autosampler vial (Waters) and dried under N2. The residue was reconstituted in borate buffer (pH 8.5) with 6-aminoquinolyl-N-hydroxysuccinimidyl carbamate (AQC) derivatisation reagent (Waters). Microdialysate samples underwent the same procedure, but without deproteination. After reaction, the vials were transferred to an autosampler tray and cooled to 10°C until the injection (1.0 µL) of the reaction mixture into the UPLC-MS/MS system. This consisted of an ACQUITY UPLC system with autosampler (Waters) coupled online with a Xevo Tandem Quadrupole mass spectrometer (Waters), and operated using Masslynx data acquisition software (version 4.1; Waters). The samples were analyzed by UPLC-MS/MS using an Accq-Tag Ultra column (Waters). The Xevo TQ was used in the positive-ion electrospray mode and all metabolites were monitored in Selective Reaction Monitoring (SRM) using nominal mass resolution. Acquired data were evaluated using Quanlynx software (Waters), by integration of assigned SRM peaks and normalization using proper internal standards. For analysis of amino acids their 13C15N-labeled analogs were used. For other amines, the closest-eluting internal standard was employed. Blank samples were used to correct for background, and in-house developed algorithms were applied using the pooled QC samples to compensate for drift in the sensitivity of the mass spectrometer with and over different batches [33]. Quality assurance of metabolite measurements was performed only reporting compounds with a QC relative standard deviation (RSD_{QC}) under 15%.

Data exploration, PKPD modeling and clustering

Outliers were detected for each metabolite using Tukeys' Test (equation 1) [34], by comparing concentrations to the range:

$[Q_1 - 3 * (Q_3 - Q_1) , Q_3 + 3 * (Q_3 - Q_1)]$, (Equation 1)

in which Q_1 and Q_3 are the lower and upper quartiles per metabolite, respectively.

1.3% of the data points were designated as outlier, and replaced by the median of the metabolite concentration of the dose group in which the data point existed. Most of the outliers came from one specific sample in the vehicle group (see figure S1). Sequential PKPD modeling approach was applied on the non-scaled metabolite concentrations, using NONMEM® version 7.3.0 with subroutine ADVAN13. Posthoc parameter estimates of a previously developed PK model were used as input for the PKPD model [35]. This model provided remoxipride concentrations both in plasma and brain extracellular fluid ($brain_{ECF}$).

A proportional error model was used in which the residual variability (RV, ε_{ijk}) follows a normal distribution with zero mean and an estimated variance (equation 2).

$$R_{obs\,,\,ij} = R_{pred\,,\,ij} * (1 + \varepsilon_{ijk}) \quad \text{(Equation 2)}$$

Criteria for model evaluation were the drop in objective function value (OFV) calculated as -2loglikelihood ratio (> 3.84, $p < 0.05$, $df = 1$), the precision of the parameter estimates (relative standard error (RSE) < 30%) and the visual evaluation of the goodness-of-fit. 44 models were developed linking the remoxipride $brain_{ECF}$ concentrations to the metabolite responses. The drug effect was described by an E_{MAX} equation (equation 3), which was coupled to the metabolite production rate (k_{IN}) in a turnover model (equation 4) as follows:

$$Drug\ effect(DE) = \frac{E_{MAX} * [C_{REM}]}{EC_{50} + [C_{REM}]}, \quad \text{(Equation 3)}$$

$$\frac{\partial R}{\partial t} = k_{IN} * (1 - DE) - k_{OUT} * R , \quad \text{(Equation 4)}$$

in which C_{REM} is the remoxipride concentration in $brain_{ECF}$, E_{MAX} is the maximal inhibition, EC_{50} is the concentration at half maximal effect, k_{IN} is the metabolite production rate (which is derived from the metabolite baseline * k_{OUT}), k_{OUT} is the metabolite elimination rate, and R is the metabolite concentration in plasma.

We identified clusters in the scaled parameters E_{MAX}, EC_{50} and k_{OUT} using the k-means method, with scaling performed according to equation 5. K-means clustering aims to minimize the within-cluster sum of squares (WCSS), which may reach a local minimum, depending on the chosen initial cluster means. Therefore, the algorithm was repeated 5000 times, and the model with the lowest WCSS was selected.

$$\tilde{P}_{ij} = \frac{log\,(P_{ij}) - \overline{log\,(P_i)}}{sd_{log\,(Pi)}}, \qquad \text{(Equation 5)}$$

in which P_{ij} is parameter value *i* for metabolite j.

A range of 4 – 10 clusters of metabolites was obtained on basis of an elbow plot (figure S2). For each candidate clustering, a PKPD model was developed estimating a single E_{MAX}, EC_{50} and k_{OUT} per cluster and a separate baseline and RV per metabolite. The best model was selected on basis of ΔOFV < 16.27 ($p < 0.001$, $df = 3$), as compared with the next candidate cluster model.

Parameter estimates for E_{MAX}, EC_{50} and k_{OUT} appeared similar between some clusters and allowed model simplification by sharing parameters among different clusters. The initial sharing was based on similarity of parameter estimates. The reduction was performed in a stepwise approach. The first step consisted of reducing three separate models each sharing only E_{MAX}, EC_{50} or k_{OUT}. In a second step, dual combinations of these models were evaluated. The third and last step consisted of testing a shared value for all three parameters. In all three steps, the reduced models were rejected if they were significantly different from the non-reduced model ($p < 0.05$).

Finally, the best model was compared to a baseline model that did not include a drug effect component (i.e. $DE = 0$ in equation 5). A ΔOFV significance threshold was calculated to be 16.00 for each single metabolite, taking into account the family wise error rate (FWER) using Bonferroni correction. The results were compared to a partial least squares discriminant analysis (PLS-DA) on the data pooled per dose group, using the R-package mixOmics [36] after log-transformation and autoscaling of the data (excluding t=0). A Variable Importance in Projection (VIP) on the first principal component was calculated for each metabolite. Metabolites with a VIP score > 1 were reported as contributing significantly to a dose response relation for remoxipride and compared to those selected from the PKPD clustering approach. The methods were compared by a weighted Cohen's kappa-analysis.

Results

PKPD models of remoxipride effect on individual metabolites

The biogenic amine analysis detected 44 metabolites in plasma with good reproducibility ($RSD_{QC} \leq 15\%$). Unfortunately, due to metabolite degradation and detection limits, the biogenic amines could not reliably be measured in microdialysate samples. The plasma metabolites showed a general dose dependent decrease from baseline (t = 0h) in the treatment groups (figure 1) with different longitudinal patterns, some of them showing a slow and others a more rapid return to baseline (figure 1). The placebo group showed

an increase from baseline for many metabolites, which we initially attempted to describe by the mathematical bateman function that previously has been used to describe such placebo response [37]. This, however, did not result in an improved description of the data as compared to a model without a placebo effect included (Bonferroni corrected $p > 0.05$).

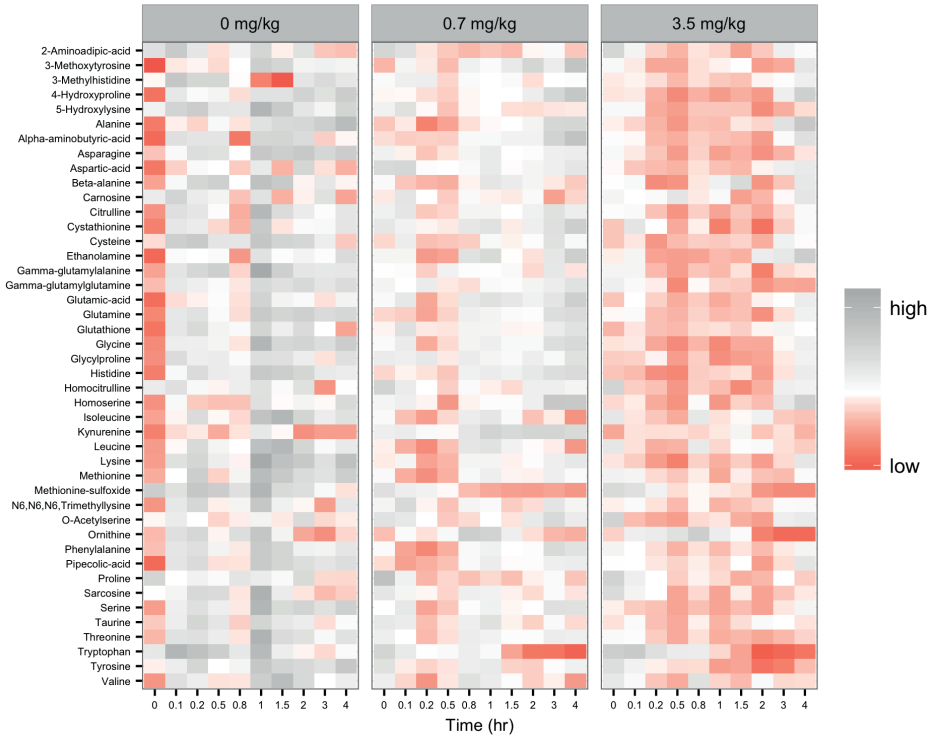

Figure 1 Heatmap showing the longitudinal response for each metabolite in the different remoxipride dose groups. Data are log-transformed and autoscaled, and mean responses are shown.

Since the metabolite responses were decreasing after treatment, the effect of remoxipride was mathematically described as an inhibition of the metabolite production rates (equations 4 & 5) for each individual metabolite, in a turnover model. The E_{MAX} for the metabolite kynurenine approached zero, indicating that remoxipride had no effect on this metabolite (figure 2). Furthermore, some metabolites showed a similar parameter pattern (e.g. glycine versus lysine), whereas others exhibited different characteristics (e.g. threonine versus tryptophan) (figure 2, indicated in pink). Particularly, the EC_{50} and k_{out} estimates were different for some metabolites (figure 2, figure S3)).

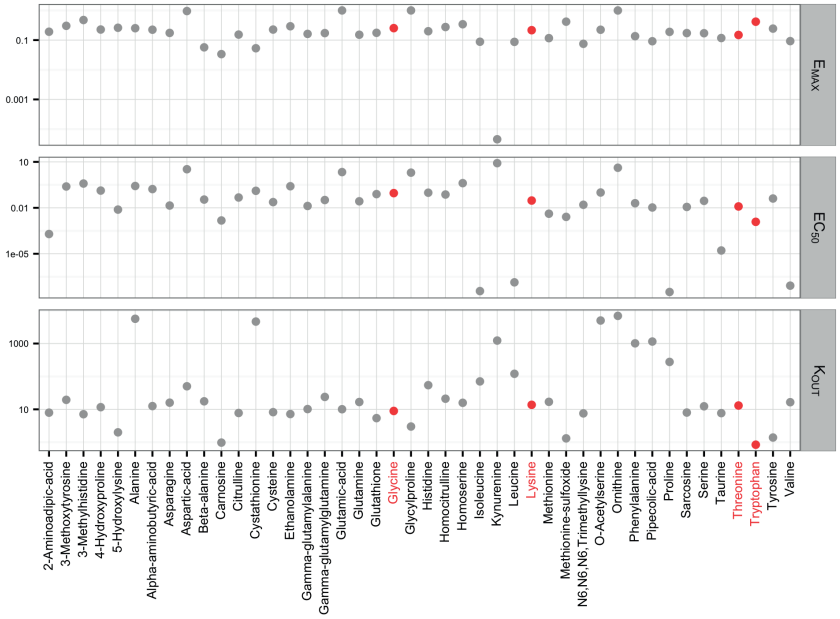

Figure 2. Parameter estimates of the 44 PKPD models describing the individual metabolite responses. The red colors are indicating examples of metabolite with similar (glycine and lysine) or distinct (threonine and tryptophan) parameter estimates.

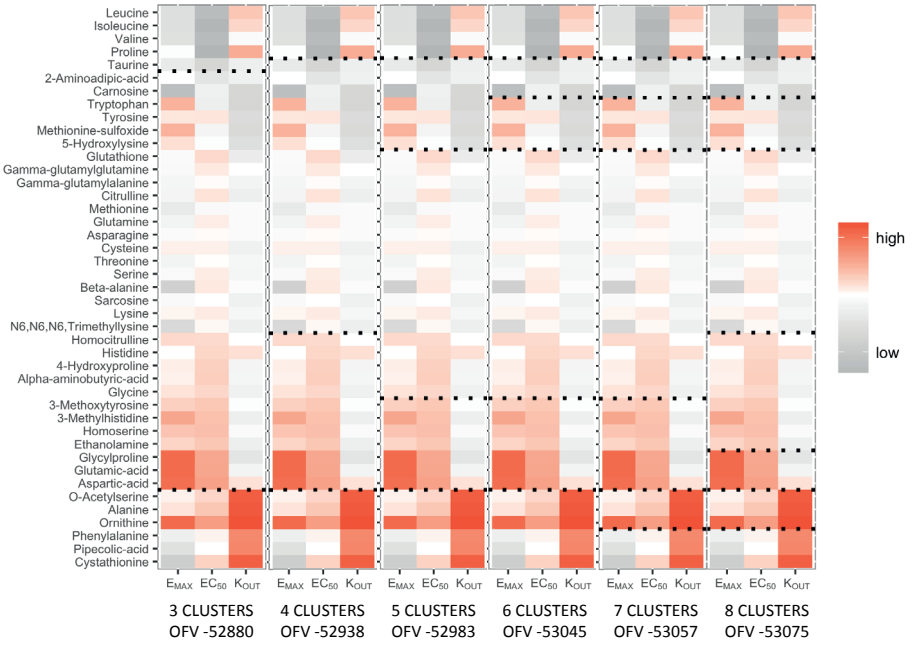

Figure 3. K-means clustering results for 3 – 8 candidate clusters. Black dotted lines indicate the cluster separation. OFV values are shown for each candidate PKPD cluster model.

PKPD models of remoxipride effect on clusters of endogenous metabolites

Metabolite clusters were identified on basis of the parameter estimates for E_{MAX}, EC_{50} and K_{OUT}. Using the multi-model k-means clustering approach and subsequent cluster-based turnover model development (see methods section), the model with 6 clusters was found to best fit the data (figure 3). This model was significantly different from the 5-cluster model (*ΔOFV > 16.27*, *p < 0.001, df = 3*), but not from the 7-cluster model (*ΔOFV < 16.27*, *p > 0.001, df = 3*).

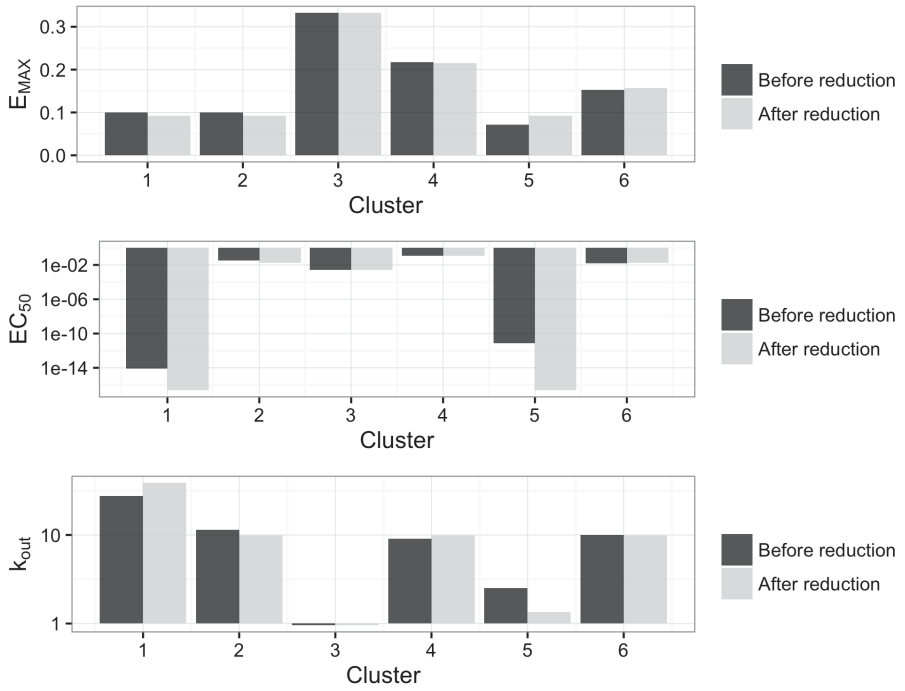

Figure 4. The effect of parameter reduction on the parameter estimates of E_{MAX}, EC_{50} and k_{OUT} were evaluated for each cluster, comparing the estimates before (black bars) and after (grey bars) reduction.

Parameter sharing led to a further simplification of the model with 6 less parameters. The more complex model was not significantly different from the simplified model (*ΔOFV < 12.59, p > 0.05, df = 6*) and the parameter estimates were highly similar (figure 4). We identified four different E_{MAX}, four different EC_{50}, and four different k_{OUT} parameters (figure 4, Table 1). The parameter estimates in cluster 1 and 5 were imprecise (Table 1) and did not show a significant effect when compared with the model not including drug effect (figure 6). Moreover, the EC_{50} approached 0 for these clusters and was therefore fixed at a value close to 0. It is concluded that a remoxipride effect could not be reliably identified. Although the kynurenine response (cluster 0) showed a possible trend in the placebo

Table 1. Parameter estimates for the PKPD cluster model describing the multiple metabolite responses in 6 different response clusters.

	Parameter	Estimate (RSE%)
Cluster 1	E_{MAX}	0.093 (7)
(4 metabolites)	EC_{50} (uM)	~ 0 (fix)
	k_{out} (h^{-1})	39 (182)
Cluster 2	E_{MAX}	0.093 (7)
(6 metabolites)	EC_{50} (uM)	0.019 (19)
	k_{out} (h^{-1})	9.9 (15)
Cluster 3	E_{MAX}	0.33 (19)
(4 metabolites)	EC_{50} (uM)	0.0027 (72)
	k_{out} (h^{-1})	0.96 (23)
Cluster 4	E_{MAX}	0.22 (23)
(7 metabolites)	EC_{50} (uM)	0.12 (43)
	k_{out} (h^{-1})	9.9 (15)
Cluster 5	E_{MAX}	0.093 (7)
(3 metabolites)	EC_{50} (uM)	~ 0 (fix)
	k_{out} (h^{-1})	1.3 (51)
Cluster 6	E_{MAX}	0.16 (6)
(19 metabolites)	EC_{50} (uM)	0.019 (19)
	k_{out} (h^{-1})	9.9 (15)

Note: cluster 0 is not included since it represented the metabolite (kynurenine) that was not affected by remoxipride.

group (0 mg/kg), this was not consistent in the other dose groups (figure 5). Parameter estimates in cluster 2, 3, 4 and 6 could be precisely determined (RSE < 30%), except for the EC_{50} in cluster 3 (RSE > 50%). The predicted centroids (i.e. the time and dose dependent average cluster response) showed good agreement with the observed centroids (figure 5). Ornithine (cluster 2) was excluded from this graph, since the effect on ornithine was in the positive direction. The single metabolite responses for ornithine and the other metabolites were reasonably to well predicted (figure S5).

Identification of potential plasma biomarkers for remoxipride effect

As indicated in figure 6 and table SI, the model including the drug effect significantly outperformed the model without drug effect for 18 metabolites ($\Delta OFV > 16.00$, *adjusted* $p < 0.05$, $df = 3$).

3 metabolites (cluster 3) showed a high impact of remoxipride (E_{MAX}/EC_{50} = 122), 13 metabolites (cluster 2 and 6) a medium impact (E_{MAX}/EC_{50} = 5 – 8), whereas 2 metabolites

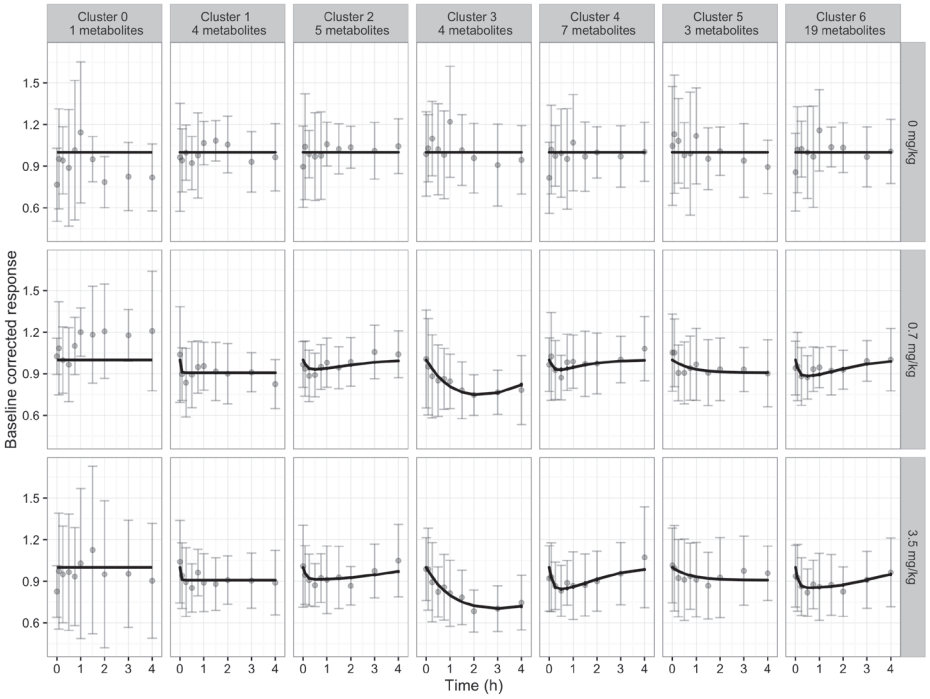

Figure 5. Goodness of fit on basis of the cluster centroids (or means) for each cluster and remoxipride dose. Predicted response is indicated by the black solid line, whereas the observed data is indicated by the grey dots (mean) and error bars (+/- standard deviation).

(cluster 4) showed a low impact (E_{MAX}/EC_{50} = 2). The turnover rate was high (9.9 /h) for cluster 2, 4 and 6, and low (0.96 /h) for cluster 3.

The PLS-DA revealed 18 metabolites with a VIP score > 1 with 13 metabolites overlapping and a Cohen's kappa of 0.38, suggesting a fair agreement between the two methods (Table 2).

Discussion

This study showed how the integration of pharmacometabolomics and PKPD modeling led to identification and significant description of 4 clusters of pharmacodynamic patterns. The model predicts the diverse longitudinal effects of remoxipride on endogenous metabolites in plasma using a clustering approach. We propose 18 metabolites as potential biomarkers of remoxipride pharmacology.

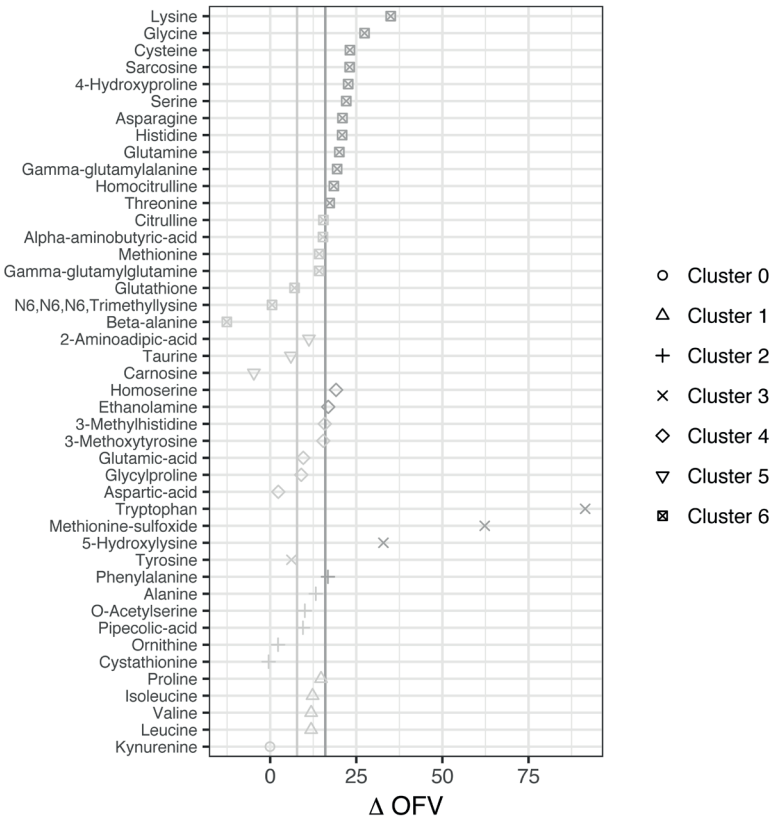

Figure 6. ΔOFV for each metabolite between the baseline model with no drug effect component and the best model with drug effect component. The light grey line indicates the significance threshold with no bonferroni correction (α = 0.05), whereas the dark grey line indicates the significance threshold with bonferroni correction (α = 0.05/44). Clusters are indicated by the different symbols.

Earlier clustering approaches have been dedicated to cluster time dependent multivariate responses. As a next step, the current method deals with the complex non-linear (concentration-effect relations are typically sigmoidal), time dependent (biological processes differ in their rates of change upon pharmacological treatment) and multivariate dose response data by step-wise integration of PKPD modeling and clustering. The model is therefore suited for predicting the multivariate dose-response relation for remoxipride with time and dose. Moreover, the model provides pharmacological meaning with the parameters that determine the concentration-effect relation (E_{MAX}, EC_{50}) and the longitudinal behavior of the response (k_{OUT}).

Many metabolites identified by the PKPD clustering method were also obtained by PLS-DA (Table 2), although PLS-DA assumes linear dose-response relations, and does not account

Table 6. Metabolites identified to show a significant dose response with PLS-DA and PKPD based clustering

Metabolite	PLS-DA[a]	PKPD based clustering[b]
3-Methylhistidine	X	
4-Hydroxyproline		X
5-Hydroxylysine	X	X
Asparagine	X	X
Beta-alanine	X	
Citrulline	X	
Cysteine	X	X
Ethanolamine		X
Gamma-glutamylalanine	X	X
Glutamine	X	X
Glycylproline	X	
Glycine	X	X
Histidine	X	X
Homocitrulline		X
Homoserine		X
Lysine	X	X
Methionine	X	
Methionine-sulfoxide	X	X
Phenylalanine		X
Sarcosine		X
Serine	X	X
Threonine	X	X
Tryptophan		X
Tyrosine	X	
Total	17	18

[a] Metabolites with a VIP score > 1; [b] Metabolites with a ΔOFV > 15.99; Cohen's kappa = 0.38

for the time dependent response behavior. Other metabolites were only identified by one of the methods. This raises the question under which conditions the methods are in agreement and when they contradict each other. As an illustrative example, homoserine shows a longitudinal dose-dependent response, which was captured by the PKPD clustering, despite the high variability. The dose-dependency was not visible if the serial data is pooled per dose group for PLS-DA analysis (figure S4, A1 vs. A2). On the other hand, glycylproline was only identified by PLS-DA. This is explained by a decrease with 3.5 mg/kg remoxipride relative to the other dose levels when pooling the data per dose group, which does not appear as a dose dependent decrease from baseline (figure S4, B1 vs. B2). Random variation in the data interfered thus both for homoserine and glycylproline with the pooled dose

response analysis (figure S4 - A2, B2, C2), and thus with PLS-DA. This suggests that the PKPD clustering method outperforms PLS-DA if random variation dominates the response. In contrast to homoserine and glycylproline, tyrosine showed a clear dose response, also as a longitudinal decrease from baseline, and was only identified by PLS-DA (figure S4, C1 vs. C2). Whereas the PKPD clustering method failed to identify tyrosine, it showed a significant response in the single metabolite model (*ΔOFV = 31.19*). The clustering thus negatively affected the fitting of the tyrosine response, while overall the 6-cluster model was identified as the best model. It is concluded that the clustering could not identify the cluster for the unique tyrosine response pattern. Further investigation did not show other cases in which the single metabolite model outperformed the cluster model.

There are clusters associated with metabolic pathways, providing a biological context of the clustering results. The branched chain amino acids (BCAA) are clustered into cluster 1, although this cluster showed no significant effect of remoxipride (figure 6). Cluster 6 is associated with the glycine, serine and threonine metabolism. Others have also found an association of D2R antagonism with this pathway, for example a decrease of glycine in plasma [17], a decrease of glycine and serine [38] as well as an increase of homoserine in brain tissue [39]. Serine is actively transported into the brain, where it is converted to glycine and phosphatidylcholine, both implicated in memory function [40]. Serine and glycine both modulate NMDA receptors, which play a main role in the glutamate pathway in the brain. Although plasma glutamate itself was not changed by remoxipride, such interaction may exist in the brain. This would not be surprising, since dopamine and glutamate systems in the brain are highly interrelated [41]. Furthermore, cluster 3 included tyrosine and tryptophan, the precursors of dopamine and serotonin, respectively. Dopamine levels are increased in different brain regions after treatment with D2R antagonists [42]. Furthermore, both tyrosine and tryptophan are converted to their neurotransmitters by the aromatic amino acid decarboxylase (AAAD) enzyme, of which the activity was increased after remoxipride and other D2R antagonists treatment [43]. The decreased tyrosine and tryptophan levels in plasma may therefore be explained by the increased uptake into the brain to refill their brain stores after increased conversion to dopamine and serotonin. These connections to pathways show how remoxipride has a potential interaction with multiple biological pathways. Further studies to these interactions should confirm the hypotheses that are generated by this study.

The different time and concentration dependent patterns in our data suggest a multilevel interaction between remoxipride and the metabolic system. It is not deducible what the exact origin of these differences is, but there are possible explanations. It might be partly caused by on-target versus off-target effects, considering the large differences in E_{MAX}/EC_{50} ratio between the clusters (table SI). Although remoxipride is very selective compared to

other dopamine D2R antagonists, it also has affinity for other receptors, for example the σ-receptors [44]. The differential patterns might also be explained by remoxipride having a potential effect in multiple tissues. The dopamine D2 receptor is not only expressed in the brain, but also in many other tissues [45]. Different tissues may have different receptor concentrations affecting E_{MAX} and EC_{50}, and different drug distribution characteristics influencing k_{OUT}. Indeed, it is likely that the k_{OUT} is determined by distribution rather than by enzymatic conversion. Typically, enzymatic conversion rates of biogenic amines are >1000 /h (BRENDA Enzyme Database, 2017), while their BBB transport rates are in the range of 0.1 – 10 /h [47], similar to the k_{OUT} values that we identified. Finally, even when bound to the same receptor in the same tissue, multiple downstream pathways might have been affected with differential time and concentration dependent patterns. This idea is clearly illustrated by the differential gene expression patterns in the liver after antagonism of the glucocorticoid receptor [23].

We are aware of limitations that are to be addressed in future studies. Unfortunately, the information on the dopaminergic pathway was limited because the analytical reproducibility was not sufficient for dopamine and its metabolite 3-methoxytyrosine. Moreover, dopamine metabolites 3,4-dihydroxyphenylacetic acid (DOPAC) and homovanillic acid (HVA), as well as the dopamine precursor L-3,4-dihydroxyphenylalanine (L-DOPA) were not measurable by the current analytical platform. Activity of the dopamine pathway in the current experiment is nevertheless illustrated by significant response of tyrosine in the single metabolite model.

Furthermore, data that we obtained on metabolite concentrations in brainECF could not be used because of assay limitations. The relation between metabolite concentrations in plasma and the brain (or CSF) is not straightforward; they do not always correlate [48–51]. Good insight into this relation is crucial for the application of blood-based biomarkers in CNS pharmacology. Simultaneous analysis of biomarker-data in brain and blood would be highly valuable in translational CNS drug development because the brain provides information on drug effects at the site of action, while blood is better accessible in humans. Moreover, such analysis would enable the separation of effects in the brain from those in the periphery. Further work should improve the application of metabolomics on microdialysate samples to enable the identification of the longitudinal biomarker response in brain and plasma simultaneously.

Taking into consideration these discussions, our analysis framework that we developed on preclinical data is also promising in a clinical context. Pharmacometabolomics is increasingly used to provide insights into between-subject variability in drug response [14]. It is similarly important, or perhaps even more so, to identify the particular causes of variable

drug responses when analyzing larger and typically more variable clinical datasets. Application of PKPD based multivariate data analysis is envisioned to increase understanding of inter-individual variability of pharmacometabolomics responses. Additionally, the current framework provides the basis for interspecies translation of pharmacometabolomics responses. Applying the principles of allometric scaling can be used to scale the clearances and rate constants, while physiological information with regard to receptor functionality can be implemented to scale the E_{MAX} and the EC_{50} parameters [52,53]. Interestingly, the metabotype is highly conserved among mammalian species [11]. It is therefore anticipated that the combination of PKPD based multivariate data analysis and interspecies scaling will improve the dose selection in early clinical development.

In conclusion, we have laid out the basis for the integration of pharmacometabolomics and PKPD modeling. The developed PKPD cluster model predicts the different biochemical responses in plasma for a range of remoxipride doses and provided comprehensive insights in its drug effects. The study design with multiple dose levels and time serial sampling, together with an analytical method that measured a large number of metabolites enabled this model-based approach that mathematically linked the PK and the multiple PD responses. Remoxipride showed 6 differential response patterns, indicating a multilevel interaction between the drug and the biochemical system. In particular, the glycine, serine and threonine pathway, as well as the precursors of dopamine and serotonin, were influenced by remoxipride. It is envisioned that PKPD clustering could serve as an initial framework for the development of mechanistic systems pharmacology models.

Acknowledgements

We thank Robin Hartman and Matthijs de Bruin for performing the surgeries and experiments and Dirk-Jan van den Berg for performing the remoxipride analysis. We thank Nelus Schoeman for the valuable discussion on the potential biological pathways involved in remoxipride pharmacology.

References

[1] Kola I, Landis J. Can the pharmaceutical industry reduce attrition rates? Nat. Rev. Drug Discov. 2004;3:711–715.

[2] de Lange EC. The mastermind approach to CNS drug therapy: translational prediction of human brain distribution, target site kinetics, and therapeutic effects. Fluids Barriers CNS [Internet]. 2013;10:12. Available from: http://www.pubmedcentral.nih.gov/articlerender.fcgi?artid=3602026&tool=pmcentrez&rendertype=abstract.

[3] Yamamoto Y, Välitalo PA, Berg D-J van den, et al. A Generic Multi-Compartmental CNS Distribution Model Structure for 9 Drugs Allows Prediction of Human Brain Target Site Concentrations. Pharm. Res. [Internet]. 2016; Available from: http://dx.doi.org/10.1007/s11095-016-2065-3.

[4] de Lange ECM, Hammarlund-Udenaes M. Translational aspects of blood-brain barrier transport and central nervous system effects of drugs: from discovery to patients. Clin. Pharmacol. Ther. 2015;97:380–394.

[5] Danhof M, Alvan G, Dahl SG, et al. Mechanism-based pharmacokinetic-pharmacodynamic modeling-a new classification of biomarkers. Pharm. Res. 2005;22:1432–1437.

[6] Hurko O, Ryan JL. Translational research in central nervous system drug discovery. NeuroRx. 2005;2:671–682.

[7] Hurko O. The uses of biomarkers in drug development. Ann. N. Y. Acad. Sci. 2009;1180:1–10.

[8] Soares HD. The use of mechanistic biomarkers for evaluating investigational CNS compounds in early drug development. Curr. Opin. Investig. Drugs. 2010;11:795–801.

[9] Morgan P, Van Der Graaf PH, Arrowsmith J, et al. Can the flow of medicines be improved? Fundamental pharmacokinetic and pharmacological principles toward improving Phase II survival. Drug Discov. Today [Internet]. 2012;17:419–424. Available from: http://dx.doi.org/10.1016/j.drudis.2011.12.020.

[10] Greef J Van Der, Mcburney RN. Rescuing drug discovery: in vivo systems pathology and systems pharmacology. Nat. Rev. Drug Discov. 2005;4:961–968.

[11] van der Greef J, Adourian A, Muntendam P, et al. Lost in translation? Role of metabolomics in solving translational problems in drug discovery and development. Drug Discov. Today Technol. 2006;3:205–211.

[12] Kaddurah-Daouk R, Kristal BS, Weinshilboum RM. Metabolomics: a global biochemical approach to drug response and disease. Annu. Rev. Pharmacol. Toxicol. [Internet]. 2008;48:653–683. Available from: http://www.ncbi.nlm.nih.gov/pubmed/18184107.

[13] Hayes RL, Robinson G, Muller U, et al. Translation of Neurological Biomarkers to Clinically Relevant Platforms. Methods Mol. Biol. [Internet]. 2009;566:303–313. Available from: http://www.springerlink.com/index/10.1007/978-1-59745-562-6.

[14] Kaddurah-Daouk R, Weinshilboum R, Pharmacometabolomics Research Network. Metabolomic Signatures for Drug Response Phenotypes: Pharmacometabolomics Enables Precision Medicine. Clin. Pharmacol. Ther. [Internet]. 2015;98:71–75. Available from: http://doi.wiley.com/10.1002/cpt.134%5Cnhttp://www.ncbi.nlm.nih.gov/pubmed/25871646.

[15] Burt T, Nandal S. Pharmacometabolomics in Early-Phase Clinical Development. Clin. Transl. Sci. [Internet]. 2016;9:128–138. Available from: http://doi.wiley.com/10.1111/cts.12396.

[16] Semmar N. Metabotype Concept: Flexibility, Usefulness and Meaning in Different Biological Populations. Metabolomics [Internet]. 2012;131–166. Available from: http://www.intechopen.com/books/metabolomics.

[17] Xuan J, Pan G, Qiu Y, et al. Metabolomic profiling to identify potential serum biomarkers for schizophrenia and risperidone action. J. Proteome Res. 2011;10:5433–5443.

[18] Kaddurah-Daouk R, McEvoy J, Baillie R a, et al. Metabolomic mapping of atypical antipsychotic effects in schizophrenia. Mol. Psychiatry. 2007;12:934–945.

[19] Bartel J, Krumsiek J, Theis FJ. Statistical methods for the analysis of high-throughput metabolomics data. Comput. Struct. Biotechnol. J. [Internet]. 2013;4:e201301009. Available from: http://www.pubmedcentral.nih.gov/articlerender.fcgi?artid=3962125&tool=pmcentrez&rendertype=abstract.

[20] Smilde AK, Jansen JJ, Hoefsloot HCJ, et al. ANOVA-simultaneous component analysis (ASCA): A new tool for analyzing designed metabolomics data. Bioinformatics. 2005;21:3043–3048.

[21] de Hoon M, Imoto S, Miyano S. Statistical analysis of a small set of time-ordered gene expression data using linear splines. Bioinformatics. 2002;18:1477–1485.

[22] Bar-Joseph Z, Gerber G, Simon I, et al. Comparing the continuous representation of time-series expression profiles to identify differentially expressed genes. Proc. Natl. Acad. Sci. U. S. A. 2003;100:10146–10151.
[23] Jin JY, Almon RR, DuBois DC, et al. Modeling of corticosteroid pharmacogenomics in rat liver using gene microarrays. J. Pharmacol. Exp. Ther. 2003;307:93–109.
[24] Déjean S, Martin PGP, Baccini a., et al. Clustering Time-Series Gene Expression Data Using Smoothing Spline Derivatives. EURASIP J. Bioinforma. Syst. Biol. [Internet]. 2007;2007:1–10. Available from: http://bsb.eurasipjournals.com/content/2007/1/70561.
[25] Westerhout J, Ploeger B, Smeets J, et al. Physiologically Based Pharmacokinetic Modeling to Investigate Regional Brain Distribution Kinetics in Rats. AAPS J. 2012;14:543–553.
[26] de Witte WEA, Danhof M, van der Graaf PH, et al. In vivo Target Residence Time and Kinetic Selectivity: The Association Rate Constant as Determinant. Trends Pharmacol. Sci. [Internet]. 2016;37:831–842. Available from: http://dx.doi.org/10.1016/j.tips.2016.06.008.
[27] Ramakrishnan R, DuBois DC, Almon RR, et al. Fifth-Generation Model for Corticosteroid Pharmacodynamics: Application to Steady-State Receptor Down-Regulation and Enzyme Induction Patterns during Seven-Day Continuous Infusion of Methylprednisolone in Rats. J. Pharmacokinet. Pharmacodyn. 2002;29:1–24.
[28] Stevens J, Ploeger BA, Hammarlund-Udenaes M, et al. Mechanism-based PK-PD model for the prolactin biological system response following an acute dopamine inhibition challenge: Quantitative extrapolation to humans. J. Pharmacokinet. Pharmacodyn. 2012;39:463–477.
[29] Derendorf H, Meibohm B. Modeling of pharmacokinetic/pharmacodynamic (PK/PD) relationships: Concepts and perspectives. Pharm. Res. 1999. p. 176–185.
[30] de Lange ECM, Ravenstijn PGM, Groenendaal D, et al. Toward the prediction of CNS drug-effect profiles in physiological and pathological conditions using microdialysis and mechanism-based pharmacokinetic-pharmacodynamic modeling. AAPS J. 2005;7:E532–E543.
[31] Danhof M, de Jongh J, De Lange ECM, et al. Mechanism-based pharmacokinetic-pharmacodynamic modeling: biophase distribution, receptor theory, and dynamical systems analysis. Annu. Rev. Pharmacol. Toxicol. 2007;47:357–400.
[32] Noga MJ, Dane A, Shi S, et al. Metabolomics of cerebrospinal fluid reveals changes in the central nervous system metabolism in a rat model of multiple sclerosis. Metabolomics. 2012;8:253–263.
[33] Van Der Kloet FM, Bobeldijk I, Verheij ER, et al. Analytical error reduction using single point calibration for accurate and precise metabolomic phenotyping. J. Proteome Res. 2009;8:5132–5141.
[34] Tukey JW. Exploratory Data Analysis. Addison-Wesley; 1977.
[35] van den Brink WJ, Wong YC, Gülave B, et al. Revealing the Neuroendocrine Response After Remoxipride Treatment Using Multi-Biomarker Discovery and Quantifying It by PK/PD Modeling. AAPS J. [Internet]. 2016; Available from: http://link.springer.com/10.1208/s12248-016-0002-3.
[36] Cao K-A Le, Rohart F, Gonzalez I, et al. mixOmics: Omics Data Integration Project. R package version 6.1.1. https://CRAN.R-project.org/package=mixOmics. 2016.
[37] Shang EY, Gibbs MA, Landen JW, et al. Evaluation of structural models to describe the effect of placebo upon the time course of major depressive disorder. J. Pharmacokinet. Pharmacodyn. 2009;36:63–80.
[38] Baruah S, Waziri R, Sherman A. Neuroleptic effects on serine and glycine metabolism. Biol. Psychiatry. 1993;34:544–550.
[39] McClay JL, Vunck SA, Batman AM, et al. Neurochemical metabolomics reveals disruption to sphingolipid metabolism following chronic haloperidol administration. J Neuroimmune Pharmacol. 2015;10:425–434.
[40] Woronczak JP, Siucińska E, Kossut M, et al. Temporal dynamics and regional distribution of [14C] serine uptake into mouse brain. Acta Neurobiol. Exp. (Wars). [Internet]. 1995;55:233–241. Available from: http://www.ncbi.nlm.nih.gov/pubmed/8713353.
[41] Javitt DC. Glutamate and Schizophrenia: Phencyclidine, N-Methyl-d-Aspartate Receptors, and Dopamine-Glutamate Interactions. Int. Rev. Neurobiol. 2007;78:69–108.
[42] Tanda G, Valentini V, De Luca MA, et al. A systematic microdialysis study of dopamine transmission in the accumbens shell/core and prefrontal cortex after acute antipsychotics. Psychopharmacology (Berl). 2015;232:1427–1440.
[43] Hadjiconstantinou M, Neff NH. Enhancing aromatic L-amino acid decarboxylase activity: implications for L-DOPA treatment in Parkinson's disease. CNS Neurosci. Ther. 2008;14:340–351.

[44] Köhler C, Hall H, Magnusson O, et al. Biochemical pharmacology of the atypical neuroleptic remoxipride. Acta Psychiatr. Scand. Suppl. [Internet]. 1990;358:27–36. Available from: http://www.ncbi.nlm.nih.gov/pubmed/1978484.

[45] Uhlén M, Fagerberg L, Hallström BM, et al. Tissue-based map of the human proteome. Science (80-.). [Internet]. 2015;347:1260419–1260419. Available from: http://www.ncbi.nlm.nih.gov/pubmed/25613900.

[46] BRENDA Enzyme Database [Internet]. 2017 [cited 2017 May 19]. Available from: www.brenda-enzymes.org.

[47] Pardridge WM. Kinetics of Competitive Inhibition of Neutral Amino Acid Transport Across the Blood-Brain Barrier. J. Neurochem. 1977;28:103–108.

[48] Jimhez-jimcnez FJ, Molina A, Vargas C, et al. Neurotransmitter amino acids in cerebrospinal fluid of patients with Parkinson ' s disease. J. Neurol. Sci. 1996;141:39–44.

[49] Lewitt PA, Lu M, Auinger P. Metabolomic biomarkers as strong correlates of Parkinson disease progression. 2017;

[50] Mans AM, Saunders SJ, Kirsch RE, et al. Correlation of Plasma and Brain Amino Acid and Putative Neurotransmitter Alterations During Acute Hepatic Coma in the Rat. J. Neurochem. 1979;32:285–292.

[51] Curzon G, Knott PJ. Effects on Plasma and Brain Tryptophan in the Rat of Drugs and Hormones that Influence the Concentration of Unesterified Fatty Acid in the Plasma. 1974;197–204.

[52] Danhof M, de Lange ECM, Della Pasqua OE, et al. Mechanism-based pharmacokinetic-pharmacodynamic (PK-PD) modeling in translational drug research. Trends Pharmacol. Sci. 2008;29:186–191.

[53] Mager DE, Woo S, Jusko WJ. Scaling Pharmacodynamics from In Vitro and Preclinical Animal Studies to Humans. Drug Metab. Pharmacokinet. 2009;24:16–24.

SUPPLEMENTARY MATERIALS

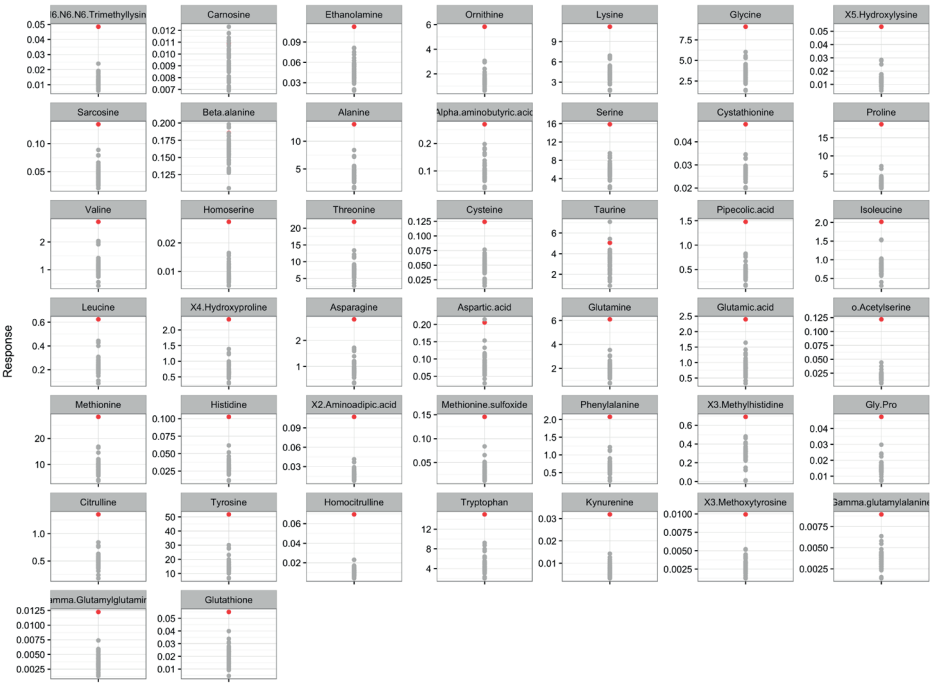

Figure S1. Investigation of the main source of outliers. The red dot represents sample R26_T15, obtained from animal 26 at 15 minutes after administration of placebo. The response is deviated from the other responses in the placebo group (black dots), indicating that this is a sample specific, and not a treatment or time point specific outlier.

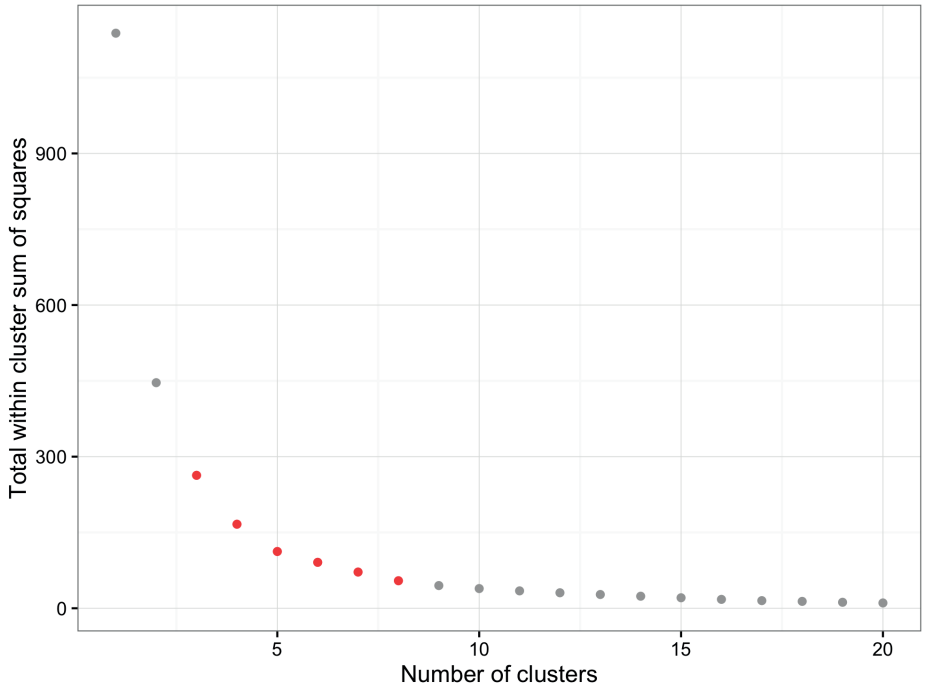

Figure S2. Elbow plot visualizing the total within cluster sum of squares (WCSS) against the number of candidate clusters for the k-means clustering. The red dots show the 'elbow' of the WCSS, indicating the range comprising the optimal number of clusters.

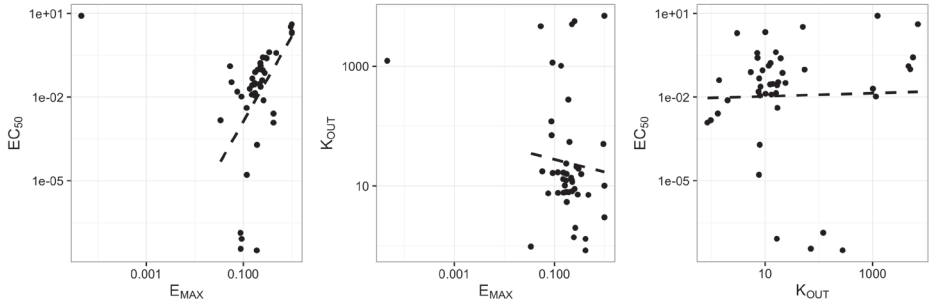

Figure S3. Correlations between E_{MAX}, EC_{50} and k_{out} (dots). Linear regression was applied to the log-transformed parameter estimates as indicated by the dashed line. Kynurenine (E_{MAX} < 0.001) was excluded from the linear regression analysis since it highly skewed the regression.

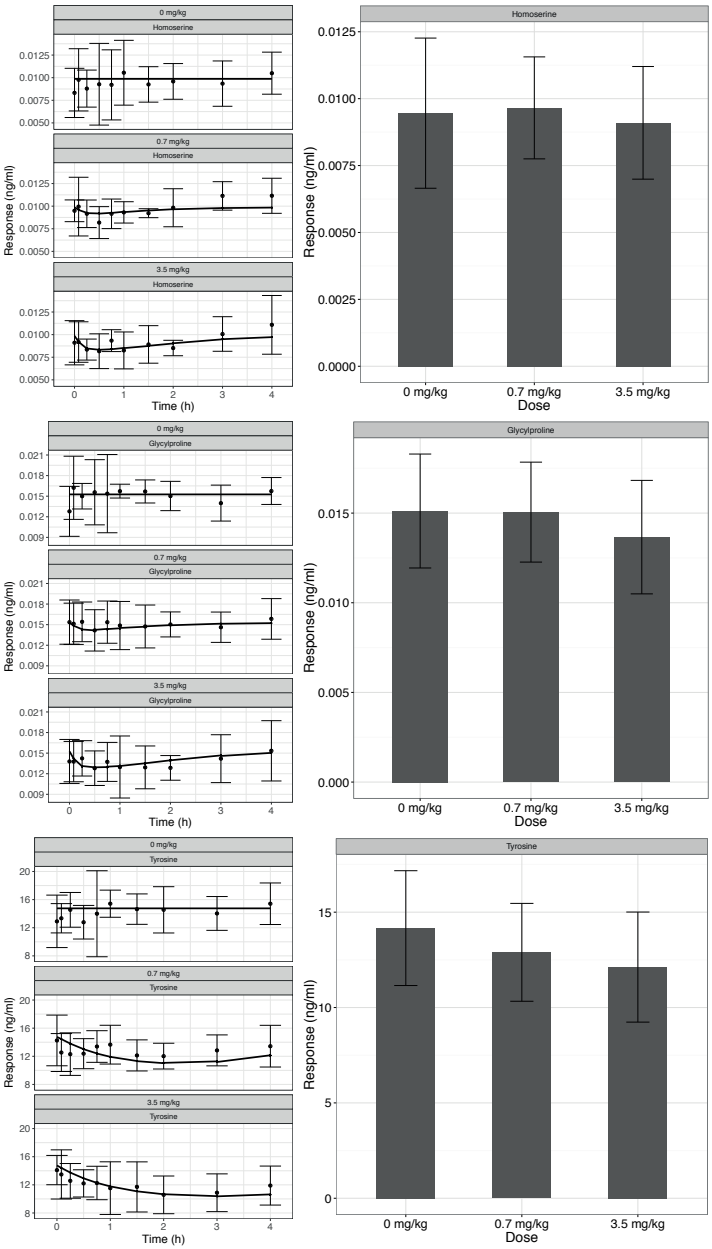

Figure S4. Dose responses for homoserine (A), glycylproline (B), and tyrosine (C), with the longitudinal responses per dose (left, 1) and the dose response (right, 2). Homoserine (A) is identified by PKPD clustering, but not by PLS-DA. No dose response is visible if the data is pooled per dose group (A2), but a longitudinal decrease from baseline is observed (A1). Glycylproline (B) is identified by PLS-DA, but not by PKPD clustering. A lower response is observed in the highest dose group (B2), but this does not appear as a longitudinal response (B2). Tyrosine (C) is identified by PLS-DA, but not by PKPD clustering. A dose response is observed (C2), which also appears as a longitudinal response (C1).

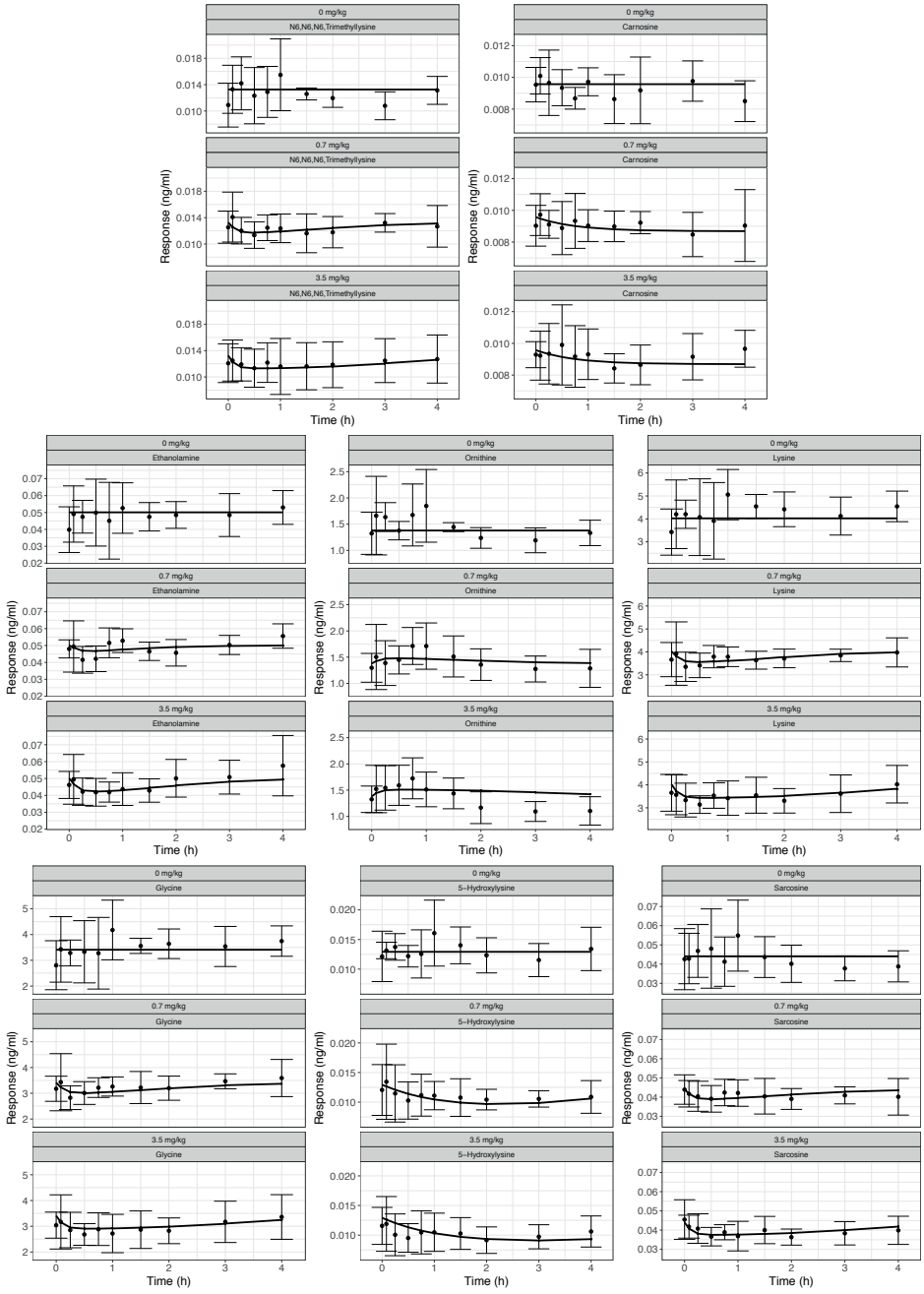

Figure S5. Goodness-of-fit for each single metabolite. Predicted response is indicated by the black solid line, whereas the observed data is indicated by the dots (mean) and error bars (+/- standard deviation).

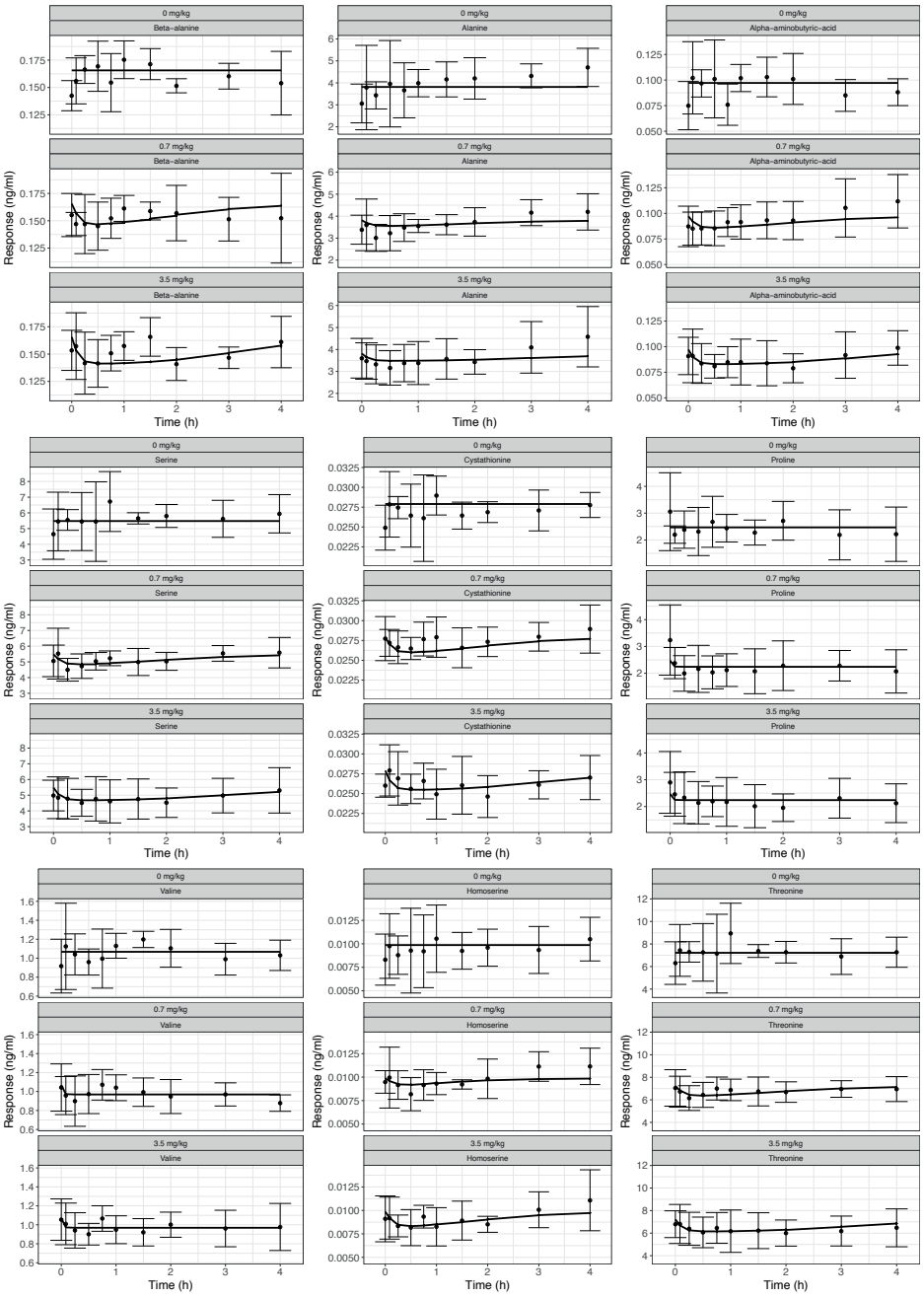

Figure S5. Goodness-of-fit for each single metabolite. Predicted response is indicated by the black solid line, whereas the observed data is indicated by the dots (mean) and error bars (+/- standard deviation).

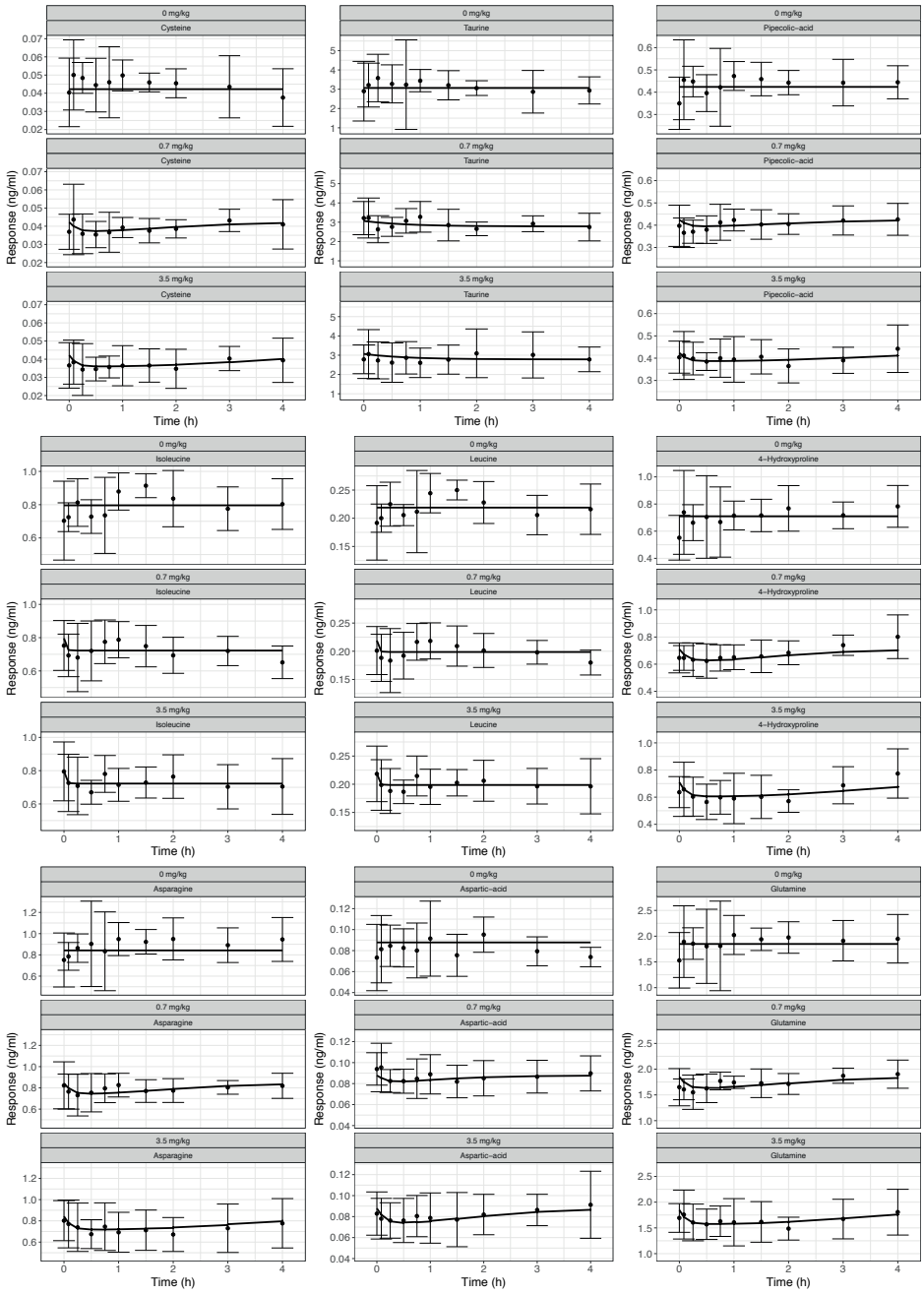

Figure S5. Goodness-of-fit for each single metabolite. Predicted response is indicated by the black solid line, whereas the observed data is indicated by the dots (mean) and error bars (+/- standard deviation).

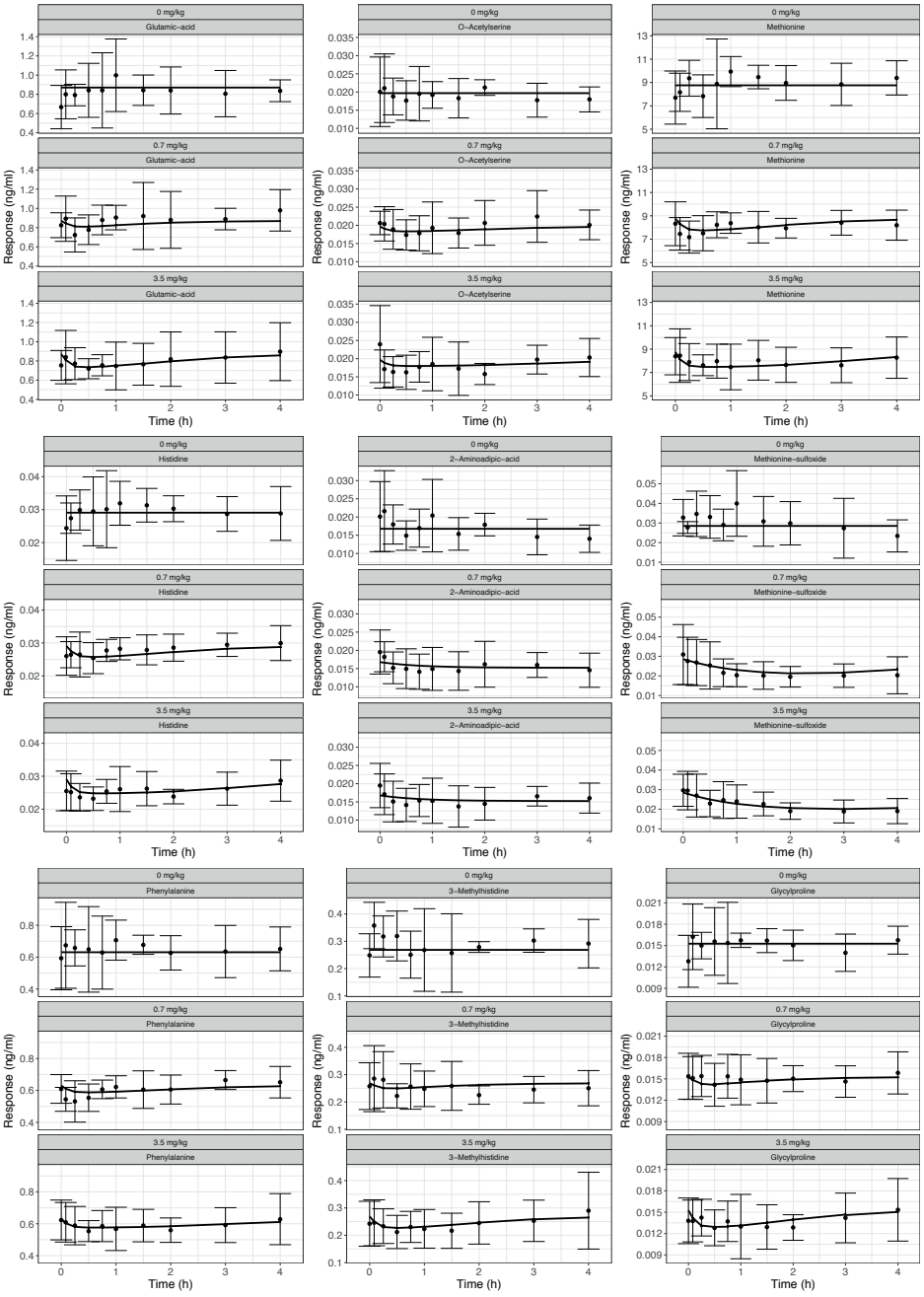

Figure S5. Goodness-of-fit for each single metabolite. Predicted response is indicated by the black solid line, whereas the observed data is indicated by the dots (mean) and error bars (+/- standard deviation).

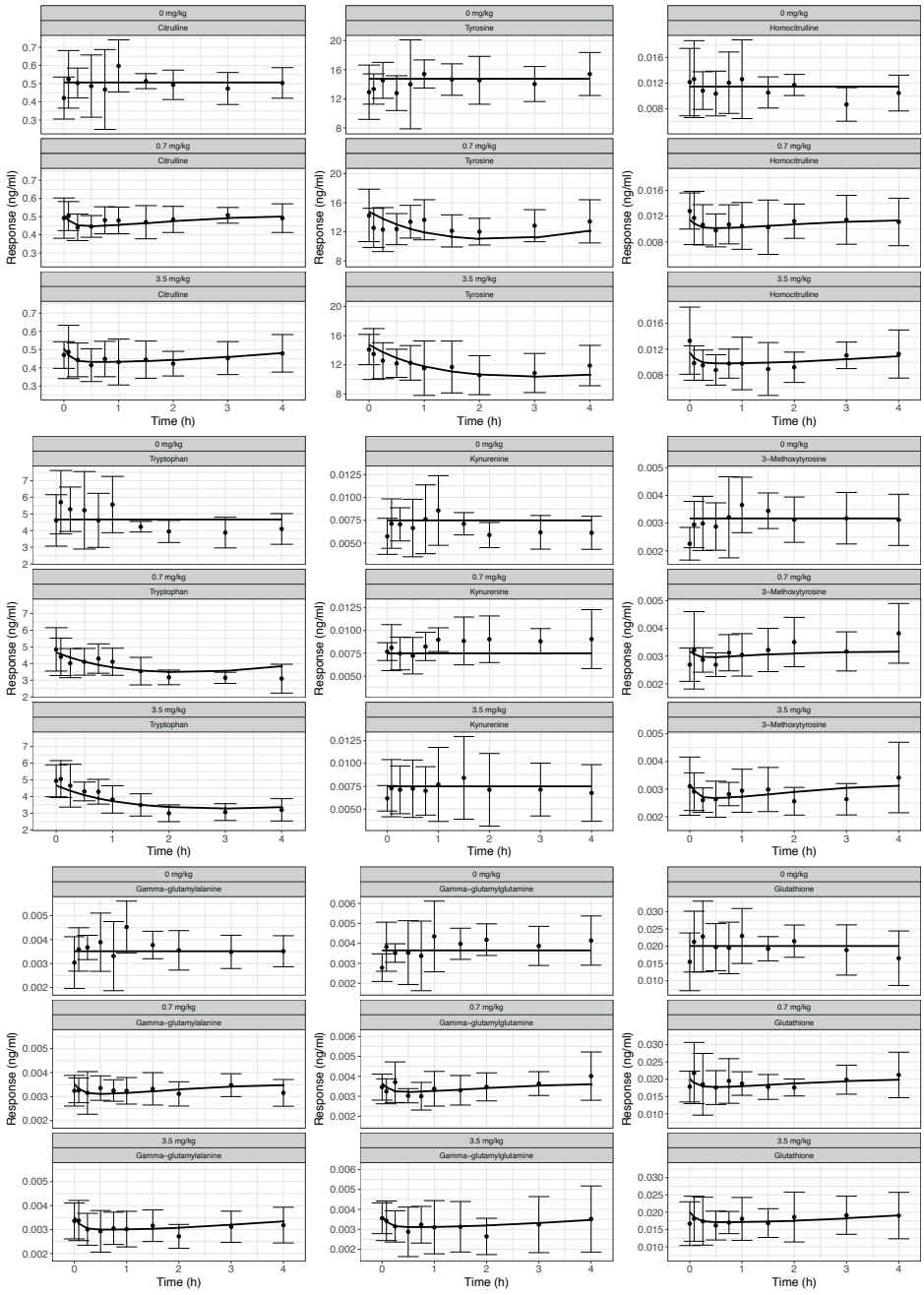

Figure S5. Goodness-of-fit for each single metabolite. Predicted response is indicated by the black solid line, whereas the observed data is indicated by the dots (mean) and error bars (+/- standard deviation).